

Scholars'
Press

Carl Fredrik Gyllenhammar

Glaciations and normal compaction in the North Sea

A critical review of currently available pore pressure methods and its input parameters

Carl Fredrik Gyllenhammar

Glaciations and normal compaction in the North Sea

FOR AUTHOR USE ONLY

FOR AUTHOR USE ONLY

Carl Fredrik Gyllenhammar

Glaciations and normal compaction in the North Sea

**A critical review of currently available pore pressure
methods and its input parameters**

FOR AUTHOR USE ONLY

Scholars' Press

Imprint

Any brand names and product names mentioned in this book are subject to trademark, brand or patent protection and are trademarks or registered trademarks of their respective holders. The use of brand names, product names, common names, trade names, product descriptions etc. even without a particular marking in this work is in no way to be construed to mean that such names may be regarded as unrestricted in respect of trademark and brand protection legislation and could thus be used by anyone.

Cover image: www.ingimage.com

Publisher:

Scholars' Press

is a trademark of

International Book Market Service Ltd., member of OmniScriptum Publishing Group

17 Meldrum Street, Beau Bassin 71504, Mauritius

Printed at: see last page

ISBN: 978-613-8-94464-5

Copyright © Carl Fredrik Gyllenhammar

Copyright © 2020 International Book Market Service Ltd., member of OmniScriptum Publishing Group

FOR AUTHOR USE ONLY

**A critical review of currently available pore
pressure methods and their input
parameters.**

-

**Glaciations and compaction of North Sea
sediments.**

By

Carl Fredrik Gyllenhammar

This thesis was submitted as the fulfilment of the requirements for the
degree of Doctor of Philosophy

Abstract

Historically pore pressure evaluation in exploration areas was based on empirical relationships between drilling parameters, wireline logs and the mud weight. Examples include Eaton's Ratio and the Hottman & Johnson Methods, which were based on data from the Gulf of Mexico. These methods are not readily transported to other areas, such as the North Sea Basin, where the sediments are different in character and where burial and temperature histories are distinctly different.

Data from several offshore North Sea wells, with high quality wireline and associated data have been analysed to determine the most appropriate method to estimate pore pressure in mudrocks. The data have led to an understanding of the key parameters for successful pore pressure estimation. The most effective method is shown to be the Equivalent Depth Method, but only where disequilibrium compaction is the source of the overpressure in the mudrocks.

Core samples from 576 British Geological Survey sites in the offshore area of the British Islands were compared with >10,000 porosities collected from the deep oceans (DSDP/ODP sites), which show that the porosities in the shallow section in the North Sea are anomalously low. The shallow section of the North Sea includes large volumes of Pleistocene-Recent sediments deposited as glacial and inter-glacial deposits. Frequency analysis (Cyclolog) of the wireline data covering this interval in several North Sea wells revealed a pattern in the relative featureless original data. Comparison with the global signature for oxygen isotopes for the same time period suggests that there have been ten cycles of ice sheet build up (Glacial period) followed by melting (Interglacial period) during the last one million years. Glacial deposits from 10 individual glacial cycles have therefore been identified in several exploration wells in the North Sea. Implications of loading/unloading of ice for the migration and trapping of hydrocarbons in the North Sea Basin are assessed.

Acknowledgements

First I must thank my supervisor, Richard Swarbrick (Dick). I met Dick first time in December 1995 in London. It was the first GeoPOP meeting I attended representing Norske Conoco. When a year later I expressed interest in doing a PhD at the university of Durham, his enthusiasm, despite my age, made what was laying ahead possible. My wife Marit and I left our jobs late 1998, we sold our house in Stavanger and moved to Durham with our two children, Elen-Martine and Fredrik.

At the university I found Dick's continues support and interest in my subject as well as the requirement to deliver regular reports to GeoPOP an assurance for continued progress. Neil Goulty was never far away to discuss any difficult equation. Both his and Dick's enthusiasm for my "ice theory" made this thesis what it is. I had also help from Fred Wollard's long experience with using principle component analysis. The last year in Durham I was lucky to share an office with Martin Traugott. He shared his long experience in pore pressure prediction as well as his own developed software PresGraf with me.

My thanks also goes to Norske Conoco, in particularly James Middleton. They supplied the well data I used as well as providing financial support for the project. Thanks go to all those from GeoPOP who were there to help and exchange ideas, Toby, Paul, Daniel, Neville, Gareth Yardley, Andy Aplin and Yunlai Yang. Finally many thanks to my new colleges at BP, for their support during the last year, Nigel Last, Mark Alberty and Mike McLean.

Table of Contents

Abstract	ii
Acknowledgements	iii
Table of Contents	iv
List of Tables	vi
List of Figures	vii
Declaration	xi
Chapter 1 Introduction	1
1.1 Background	2
1.2 Data	3
1.3 Introduction	7
1.4 Pressure, the basic concepts	11
1.5 Aims and layout of thesis	14
Chapter 2 Pore Pressure Evaluation Concepts and definitions	16
2.1 Definition	17
2.1.1 Mudrock porosity	18
2.1.2 Different porosity evaluation equations	18
2.1.3 Normal compaction curve and trend lines	23
2.1.3.1 Athy-type relationship	24
2.1.3.2 Soil mechanics relationship	25
2.1.3.3 Athy - Soil mechanics: how are they different	25
2.1.4 Vertical versus mean effective stress	28
2.2 Pore Pressure Calculation Methods	29
2.2.1 Vertical Methods	30
2.2.1.1 Equivalent depth method	30
2.2.1.2 Harrold method	32
2.2.1.3 Explicit method using the resistivity log	33
2.2.2 Horizontal methods	35
2.2.2.1 Eaton Method	35
2.2.2.2 The pore pressure calculation program; PresGraf	37
2.2.2.2.1 PresGraf normal compaction trend	37
2.2.3 Seismic	40
2.2.4 ShaleQuant	41
2.2.5 Principle Component Analysis	41
2.3 Drilling parameters	46
2.3.1 Real time data	48
2.3.2 D'exponent	48
2.3.3 Torque	54
2.3.4 Hydraulics	55
2.3.5 Bit type and wear	55
2.3.6 Lagged data	56
2.3.6.1 Gas	56
2.3.6.2 Cuttings and Cavings	58
2.3.6.3 Mud temperature in and out	58
2.3.6.4 Mud resistivity in and out	58
2.3.7 Mud chemistry and mud-formation chemical reactions	59
Chapter 3 Comparison of different pore pressure methods using a North Sea well	60
3.1 Introduction	61
3.2 Pore pressure evaluation of well 1/6-7 in the North Sea, Norwegian sector	61
3.2.1 Pore pressure evaluation while drilling (wellsite)	62
3.2.2 The Post-well analysis	63
3.2.2.1 Tertiary	67
3.2.2.2 Chalk	67

3.2.2.3	Jurassic.....	67
3.3	Normal Compaction in the North Sea.....	69
3.3.1	Palaeocene and Lower Eocene.....	75
3.3.2	Normal compaction from resistivity data.....	76
3.4	Wireline log pore pressure calculation.....	78
3.5	Comparing the North Sea with the Gulf of Mexico Basin.....	86
3.6	Vimto#1 and #2.....	87
3.7	Summary and conclusions.....	93
Chapter 4	The impact of the Glaciation on the Normal compaction in the North Sea.....	96
4.1	Introduction.....	97
4.2	Glacial history.....	99
4.2.1	The Neogene – Pleistogene sedimentary succession.....	102
4.3	Tills.....	103
4.4	Mudrock porosities.....	104
4.5	Oxygen isotope data.....	106
4.6	Time series frequency analysis (CycloLog).....	108
4.7	Ice loading and pore pressure.....	112
4.8	Subglacial water flow.....	118
4.8.1	Resistivity log response.....	121
4.9	Hydrocarbon migration.....	122
4.10	Erosion of the Scandinavia during Quaternary.....	123
4.11	Conclusions.....	124
References:	126
Appendix 1	136
Appendix 2	145
Appendix 3	155

List of Tables

Table 2-1 Eigenanalysis of the correlation matrix	42
Table 2-2 A list of measurements that can be used to interpret the shale pore pressure.	47
Table 2-3 Eigenanalysis of the correlation matrix	52
Table 4-1 BGS sits and exploration wells.....	105
Table 4-2 The flow rates are calculated assuming hydrostatic pressure in the aquifer underlying the aquitard.	120

FOR AUTHOR USE ONLY

List of Figures

Figure 1.1 The wireline log plot of well 1/6-7 from seabed to 2000m.....	4
Figure 1.2 The wireline log plot of well 1/6-7 from 1900 to 4000m.....	5
Figure 1.3 The wireline log plot of well 1/6-7 from 3000 m to 4995 m (TD).....	6
Figure 1.4 Schematic of wireline logging. The lithological column to the right is a schematic of a pressure probe (RFT) being used to measure the pore pressure in permeable sandstone.	9
Figure 1.5 Pressure plotted against depth in a fictional well. The effective stress is equal to the overburden pressure minus the pore pressure and the overpressure is equal to the pore pressure minus the hydrostatic pressure.....	12
Figure 1.6 The Figure to the right shows how a pressure versus depth plot (left, Figure 1.5) becomes presented as pressure gradient versus depth.	14
Figure 2.1 a,b,c,d. 1a porosity variation as a function of sonic velocity. B, porosity versus bulk density. C, the sensitivity to pore water density. D, the sensitivity to matrix density.....	20
Figure 2.2 Log derived porosities in well Nor-1/6-7 Norway. The low porosity interval from 3261m to 4346m depth is the Cretaceous Chalk. The values are listed in Appendix 1.	23
Figure 2.3 Comparison of porosity with effective stress for the Athy and the SM equations. Initial porosity (sea floor porosity) for Athy is 0.7 (70 %) while the porosity at 100 kPa (approximately 100 meters below sea floor) is 0.66 (66 %) The compaction factors a_{re} for Athy; 0.00008 and SM; 0.74.	26
Figure 2.4 The relationship between porosity, solidity and void ratio is shown. The y-axis is the compaction as a length reduction. It is assumed that a confined volume is compressed beginning with a void ratio of four.....	27
Figure 2.5. Porosity from a pseudo well is plotted versus depth. Integrating the density log and subtracting the hydrostatic pressure calculate the effective stress. The two normal compaction curves are coming from Figure 2.3.	30
Figure 2.6 Porosity from a pseudo well is plotted versus mean effective stress. The two normal compaction curves are coming from Figure 2.3. See text for an explanation for the equivalent effective stress method.	32
Figure 2.7 Comparing the porosity derived from the sonic, density and neutron log with the resistivity derived using the equation 1.37 proposed by Alixant and Desbrandes (1991).	34
Figure 2.8 The PresGraf normal compaction trend to the left compared with the Athy normal compaction curve (Figure 2.3) to the right.	39
Figure 2.9 Scree plot of the eigenvalue of each principal component of the PCA of the wireline logs.....	43
Figure 2.10 a, b, c and d. The plots to the left (a and c) are cross sections through data perpendicular to PC1, PC2 and PC3. b and d show the loading values with respect to the different principal components.	44
Figure 2.11 a and b. PC1 versus depth in blue and the sonic travel time in green.	46
Figure 2.12 The plot shows the d' exponent and the corrected d' exponent versus depth. The straight lines are trend lines representing one particular pressure gradient (one mud weight).	49
Figure 2.13 Cross plot of the d' exponent versus the sonic travel time, well N 1/6-7. It suggests a good relationship between the sonic log and the d' exponent in the Tertiary section (pink squares). The correlation is less obvious in the Jurassic (yellow triangles). There is no correlation in the Chalk.	50

Figure 2.14 Cross plot of the d'exponent versus the resistivity log. The plot show no correlation.	51
Figure 2.15 Scree plot of the eigenvalue of each principal component of the PCA of the drilling parameters	53
Figure 2.16 a, b, c, d. The plots to the left (a and c) are cross sections through data perpendicular to PC1, PC2 and PC3. b and d show the loading values with respect to the different principal components.	53
Figure 2.17 a, b and c. PC1 versus depth with the standardized log porosity overlaid in Figure b and the normalized sonic travel time in Figure c	54
Figure 3.1 The corrected d'exponent plotted versus depth with a normal trend line overlaid in green. Normally new trend lines will be added paralleling the green line each time a new bit is put on the drill string. The new line will represent the actual MW. An alternative trend line is suggested in red. That trend line will also result in a reasonable calculated pore pressure at the target of interest (i.e. 4200 to 4800 m).	63
Figure 3.2 The sonic velocities in the shale sections plotted against depth on a semilogarithmic graph. The yellow line is the best visual fit trend line.	65
Figure 3.3 A comparison of the calculated pore pressure from the d'exponent (blue dots) and the sonic velocity calculated pore pressure.	66
Figure 3.4 Shale velocities from the wells in Figure 3.2 compared with the wells used by Hansen (1996). The Figure to the left has a logarithmic X-axis. At such a plot the Athy type normal compaction trend become a straight line. On the plot to the right it is much more obvious that the well used in this study are different from the one used by Hansen (1996).	70
Figure 3.5 Porosity data from 10000 DSDP/ODP mudrock samples. ODP site #336 is in the deep water Norwegian Sea. The yellow curve is the suggested normal compaction trend drawn through the data set.	71
Figure 3.6 Compaction trends as void ratio versus effective stress. All the different trends that have been tested in this chapter are overlaid. The PresGraf (in blue) is an approximation as the real curve is proprietary data to BP.	72
Figure 3.7. Different wireline methods to calculate the volume of clay are compared in well N 1/6-7. The red dot are Vcl from using the GR log, the blue dots from the neural network (ShaleQuant and the green dots the neutron and density log.	74
Figure 3.8 Twenty-six wells in 5 offshore areas and 4 onshore fields (MacGregor, 1965). The pink line is a suggested normal trend for the Gulf of Mexico.	77
Figure 3.9 Pore pressure in mega-Pascal versus depth in meters. The green solid line is the overburden and the blue solid line is the hydrostatic pressure. The equivalent depth method calculated pressure is in blue dots while the orange is the University of Durham method. The dashed black curve is the operator's interpretation while the olive solid line is the mud weight. The red crosses are the RFT direct pore pressure measurements.	79
Figure 3.10 Pore pressure in mega-Pascal versus depth in meters. The green solid line is the overburden and the blue solid line is the hydrostatic pressure. The Eaton equation with the sonic log as input (red dots) compared with the Equivalent depth method with the porosity as input (blue dots). The red crosses are the RFT direct pore pressure measurements. The values are listed in Appendix 2.	82
Figure 3.11 Pore pressure in mega-Pascal versus depth in meters. The green solid line is the overburden and the blue solid line is the hydrostatic pressure. The Eaton equation in red dots compared with the Equivalent depth method in solid blue,	

both with the sonic log as input. The red crosses are the RFT direct pore pressure measurements. The values are listed in Appendix 2.....	83
Figure 3.12 Pore pressure in mega-Pascal versus depth in meters. The green solid line is the overburden and the blue solid line is the hydrostatic pressure. The Equivalent depth method tested with two different normal trends. The Athy equation used by the operator of well Nor-1/6-7 (blue dots) versus the DSDP-ODP based trend (red dots).The red crosses are the RFT direct pore pressure measurements. The values are listed in Appendix 2.....	83
Figure 3.13 The shale porosity (red solid curve to the right) and the shale travel time (green solid line to the right) versus depth in the Jurassic section. The x axis is in % for porosity, $\mu\text{sec}/\text{ft}$ for the sonic log. The curves to the left of the overburden (strait solid green line) is in MPa. Between the overburden and the hydrostatic pressure (left most solid blue) are from left the pore pressure calculated using the sonic log as input (blue curve) then with porosity as input (orange curve). The values are listed in Appendix 2.....	84
Figure 3.14 Figure 3.13, the pressure transition zone from 4850- 4890 meters. The values are listed in Appendix 2.....	84
Figure 3.15 Pore pressure in mega-Pascal versus depth in meters. The green solid line is the overburden and the blue solid line is the hydrostatic pressure. The Eaton equation with the resistivity log as input (green dots) compared with the Eaton sonic (red dots). The red crosses are the RFT direct pore pressure measurements. The values are listed in Appendix 2.....	85
Figure 3.16 Depiction of salt features in the area around the basin. The local depocenters are termed mini-basins (Yardley and Couples, 2000).....	87
Figure 3.17 Comparison of the NRG derived shale porosity versus permeability curves, with some basin modelling default curves. A range of clay-fractions are shown, from 20% to 80% (Yang and Aplin, 2000).	89
Figure 3.18 Comparison of the GeoPOP derived shale compaction curves with some basin modelling default curves. A range of clay fractions are shown, from 20% to 80% (Yang and Aplin, 1999).....	90
Figure 3.19 Pore pressure prediction for Vimto #2. The blue curve is the pore pressure calculated using the Eaton method and the shale sonic velocity as input. The red line is pore pressure using the equivalent depth method. The pink diamonds are the MDT pressure points. The red line to the left is the overburden. The values are listed in Appendix 3.....	91
Figure 3.20 The reservoir section for well Vimto#2. The MDT pressures are generally 50 to 100 psi higher than the calculated shale pressures.	91
Figure 3.21 The red curve is the pore pressure calculated from a 2-D model allowing for lateral transfere (Yardley and Couples, 2000).	92
Figure 4.1 A curve showing the variation in oxygen isotope composition of the sea-water for the last 6 million years. The oxygen isotope data are based on foraminifera from three boreholes near the coast of Ecuador (Shackleton et al., 1990; Shackleton et al., 1995.....	98
Figure 4.2 Reconstruction of the Scandinavian and British Ice Sheet during a glacial stadial (after Hughes, 1998). The maximum ice thickness onshore was 2600 m and the maximum thickness in the offshore North Sea was approximately 1600 m	101
Figure 4.3 Porosity versus depth. A compilation of core measurements and wireline calculated porosities.....	106

Figure 4.5 To the left is the oxygen isotope data shown in Figure 4.1. To the right is the GR log followed by the filtered GR log from well Nor-1/3-2. The third curve is picks representing sudden changes in the cyclicity of the filtered GR curve. The third curve show peaks, positive or negative representing sudden transitions from high to low GR value, shown as a negative peak (to the left). The opposite results in a positive peak. The last curve is the integration of previous curve. These curve were output from CYCLOGLOG*. This curve represents the cumulative difference between the predicted log values and the actual log values. Breaks in the cyclicity succession may be related to missing sections or abrupt changes in sedimentation rates. A large positive peak could be a condensed section. 109

Figure 4.6 Correlation of five wells drilled in the southern part of the Norwegian sector using CycloLog software. The distance from Nor-1/3-2 to Nor-2/11-7 is about 100 km (60 miles). The cycles are compared on the left with oxygen isotope signature (See text). 111

Figure 4.7 The four maps above present the palaeo-coastline for each subsequent crustal motion model. It is important to note that large parts of the North Sea were dry land after the last deglaciation, in each case for a period of several 1000 years. 113

Figure 4.8 The figure to the left show a typical pore pressure profile in the North Sea with no seawater just prior to a glaciation. The sand at 2000 meters subcrop to seafloor and has therefore hydrostatic pressure. During glaciation of the North Sea the overburden pressure and the hydrostatic pressure increase with a pressure equivalent to the weight of the ice-sheet. If the sand subcrops under the ice-sheet the pore pressure will also increase in the sand. But if it subcrops outside the ice-sheet, its pore pressure will only vary as much as the sealevel changes. 114

Figure 4.9 The profile B-B' shown on Figure 4.7. It show that the maximum subsidence was in the centre of the Baltic Sea of more than 400 metres, while it was potentially uplift in the North Sea (Milne et al., 1999, Mitrovica et al., 1994, Tushingham, A.M., 1991)..... 116

Figure 4.10 Resistivity curves from the North Sea compared with Gulf of Mexico. The graph to the left is raw data while the raw resistivity curves have been temperature corrected on the graph to the right. 122

Declaration

The content of this thesis is the original work of the author (other people's work, where included, is acknowledged by reference). It has not been previously submitted for a degree at this or any other university.

Carl Fredrik Gyllenhammar
Durham
September 2003

FOR AUTHOR USE ONLY

Copyright

The copyright of this thesis rests with the author. No quotation from it should be published without his prior written consent and information derived from it should be acknowledged.

Chapter 1 Introduction

FOR AUTHOR USE ONLY

1.1 Background

Fifteen years ago, most pore pressure studies were undertaken solely for safety aspects in the design and drilling of exploration wells. As the need for accurate pore pressure evaluation is growing due to its general application in exploration studies such as hydrocarbon migration studies, more accurate methods founded on sound physical principles, and not just empirical observations, are needed.

Pore pressure estimation is a particular challenge in the North Sea on account of the complex tectonic and sedimentological history of the region, where the highest overpressure (pore pressures above the normal, hydrostatic pressure) are found in Jurassic and Triassic reservoir sandstones. The presence of a thick Chalk section as well as a variety of mudrock types, including a kerogen-rich petroleum source rock, challenge standard practices for pore pressure evaluation which were, in many cases, developed in the Gulf of Mexico where the rocks are younger and exclusively siliciclastic (sandstone, siltstones and shale mudrocks). The late history (Pleistocene-Holocene) of the North Sea has involved ice loading and the deposition of glacially-derived sediments which add a further component of complexity to the stress and fluid history of North Sea sediments.

The availability of a very high quality set of well data from the Norwegian North Sea (Central Graben) provided impetus for this project which was designed to test current methods of pore pressure prediction, assess the impact of a late ice-loading and unloading history and apply new technology on mudrock compaction (being concurrently developed in the GeoPOP research group – see below).

There are a number of complementary data which can be used for pore pressure evaluation including basin modelling, seismic velocities, wireline logs and drilling parameters. Each requires different data input and interpretation requirements. In this thesis the emphasis is for pore pressure evaluation using wireline logs. The response from the drilling parameters was used as an independent control.

The thesis was funded by Norske Conoco in Norway and the work was included as part of GeoPoP. GeoPoP (GEOsciences Project into OverPressure) was a joint research project involving University of Durham, Newcastle University, Heriot Watt University and industrial sponsors such as major oil companies like BP, Amoco, Statoil, Norsk Hydro, Phillips, Conoco, etc. The aim of GeoPOP was to explain how pore pressures evolve in mudrocks and to evaluate and develop new methods to predict and calculate the pore pressure in these sediments.

1.2 Data

Norske Conoco made most of the data available, consisting of wireline data from exploration wells. The most important well was 1/6-7, drilled by Norske Conoco in 1989, which is classified as a high pressure (>10,000 psi) and high temperature (>350°F) (HPHT) well. In addition to well 1/6-7 were a number of offset wells in the southern part of the Norwegian shelf. The data set included also some wells from Haltenbanken and the Barents sea. Well 1/6-7 has high quality wireline and mud logging data particularly with respect to testing pore pressure prediction and calculation methods (Figure 1.1, 1.2 and 1.3).

GeoPOP provided the data from the Gulf of Mexico. Data from the shallow coring project by British Geological Survey (BGS) were provided by BGS. Data from the Ocean Drilling Project (ODP) are freely available on the Internet and were downloaded free of any charge.

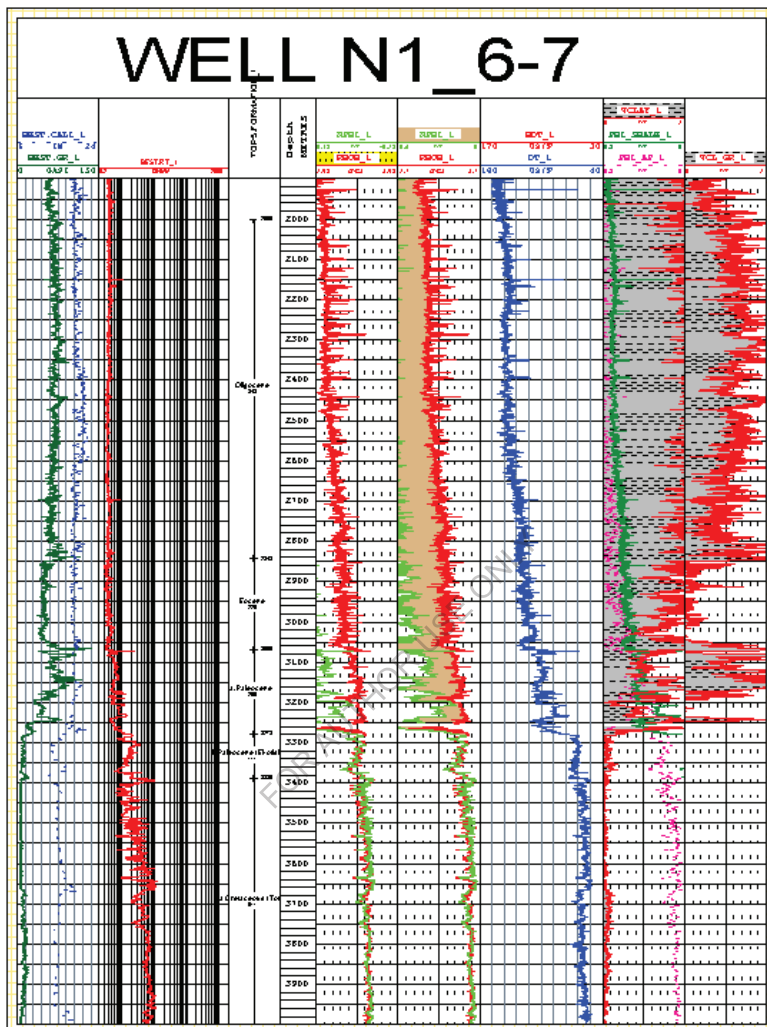


Figure 1.2 The wireline log plot of well 1/6-7 from 1900 to 4000m.

1.3 Introduction

In exploration drilling operations pressure from the circulating drilling fluid (mud) is used to prevent the pore fluid in the porous rock entering the borehole. The pressure from the mud at a particular depth is a function of the average density ($MW = \text{Mud Weight}$) and the vertical height of the column from that depth to the surface. In low permeability formations, such as mudrocks, the formation can cave into the wellbore through tensile failure if the pore pressure is higher than the counter pressure from the mud. The industry has a long history of establishing empirical relationships between drilling parameters such as the rate of penetration and the gas measured in the returning drilling fluid to the pore pressure in the mudrocks. The uses of drilling parameters are very subjective and prone to large uncertainties. The pressure can also be calculated indirectly from petrophysical measurements. Petrophysical data can be acquired while drilling or after drilling a section. In the former case the petrophysical sensors are placed behind the drill bit in operations known as Logging While Drilling (LWD) or Measurement While Drilling (MWD). When data is acquired once drilling has been completed, the petrophysical sensors are lowered down the hole suspended from a wire (wireline logging) and readings taken by the tools while being reeled back up. The pore pressures in the reservoir rocks with high permeability are measured directly using a wireline tool with a pressure gauge. A cylindrical probe with a small aperture is hydraulically forced into the formation (Figure 1.4) and the tool remains at the location until the pressure stabilizes between the inside of the tool (where the pressure gauge is located) and the formation (where the probe has been extended). The pressure is recorded as pressure vs time. The most common trade acronyms for these tools are RFT (Repeat Formation), FMT (Formation multi-tester) or MDT (Modular Dynamics Tester). In mudrocks where permeability is very low, this tool cannot be used due to the time it will take for pressure to stabilize. Direct pressure measurements are also recorded when a hydrocarbon zone is tested, called a Drill Stem Test (DST).

The accompanying petrophysical measurements collected at the same time as the pressure tests include sonic, velocity, neutron porosity, density, and resistivity (unless you intended to list something else). These sensors are all calibrated for the porous formation and will tend to give erroneous reading if any clay minerals are present.

The challenge is therefore to use these measurements in mudrocks with low permeability and high clay content. During compaction of compressible sediment, such as mudrock, water is expelled and the porosity decreases. If the free water which needs to be expelled to maintain equilibrium with the imposed stresses cannot drain out of the system, the porosity will not decrease, with the result that the pore pressure increases above the hydrostatic pressure. Porosity cannot be measured directly in a borehole. The porosity is calculated indirectly from the sonic velocity, neutron porosity, density or the resistivity measurement, or a combination of these measurements. The effective or inter-granular stress is then calculated using a relationship between the porosity, the normal compaction trend and the total lithostatic stress (overburden stress).

A variety of empirical relationships have been developed for calculating mudrock porosity from different log responses. Typically, a stress-porosity relationship is not used directly, but instead porosity is compared against a normal compaction trend, which would be the porosity against depth for the location in question assuming a 'normal' pressure profile equivalent to the hydrostatic head of a water column. In this work it will be shown that the normal compaction trend often yields the biggest uncertainties in calculating the pore pressure in mudrocks.

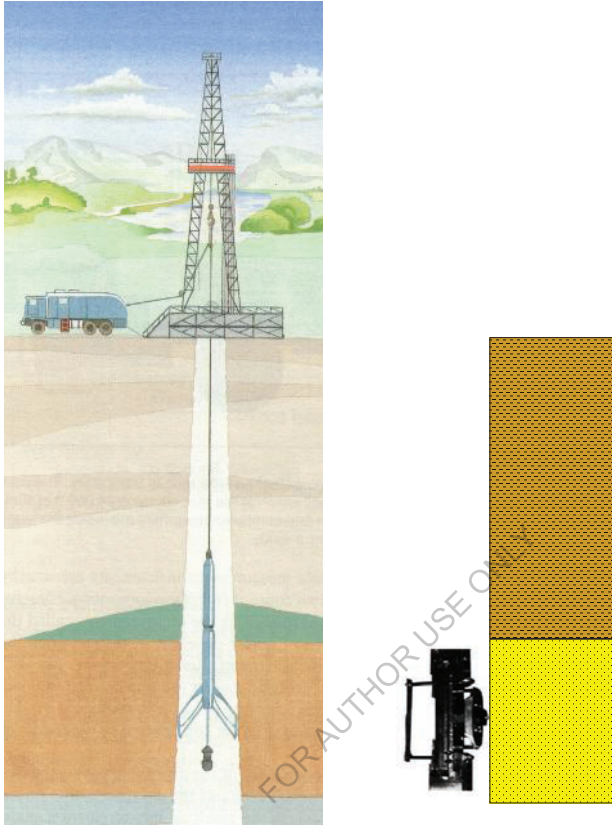


Figure 1.4 Schematic of wireline logging. The lithological column to the right is a schematic of a pressure probe (RFT) being used to measure the pore pressure in permeable sandstone.

Having inferred mudrock porosity from logs and computed or established a normal compaction trend of expected porosity for normal pressure, the final step is to find a relationship quantifies the pore pressure magnitude associated with a mismatch between the estimated mudrock porosity from log response and the normal compaction trend.. This transform or equation might be based on physical principles, such as the equivalent depth (or effective stress) method, or empirical relationships, such as the Eaton's method. It will be shown that the transform method used for calculating the pore pressure is less important than the choice of normal compaction trend.

The initial goal for this research was to establish a new method to calculate the pore pressure in mudrocks as a function of petrophysical measurements. During the course of this research it became apparent that the classical equivalent depth method is a reliable equation and it would be of limited value to attempt an improvement to it. Also, the porosity of the mudrocks can be reliably calculated from a combination of the available wireline logs. A sensitivity study shows clearly that the biggest uncertainty is the normal compaction curve. Eaton (1975) summarized it best: "The methods used to establish normal trends vary as much as the number of people who do it".

A normal compaction curve represents the reference trend describing the compaction behaviour of sediments which are normally pressured. The compaction (porosity loss involving expulsion of fluids) is caused by increases in vertical and /or horizontal stress. Conventional pore pressure prediction uses the normal compaction curve to estimate the magnitude of overpressure. Data from which normal compaction curves are derived include shallow buried sediments of the same age and lithology, or published compaction relationships. For example, Hansen (1996) examined three wells in the North Sea where he assumed that the mudrocks have normal pore pressure. He established a relationship between the sonic travel time and the mudrock porosity used in this research. Other approaches are based on laboratory measurements of compaction such as by Skempton (1970) where he showed a relationship between compaction and the volume of fine-grained material in the samples. The shortcoming of that approach is that the relationship does not take into account the different compaction behaviours of clay minerals such as montmorillonite versus fine-grained quartz, (K. Bjorlykke (2001) personal oral commun.).

This research shows that it is unlikely that any useful normal compaction trend can be established in the North Sea due to **recent glacial events**. The glacial tills left by a earlier glacial event have been overlooked for many years. The nature of these sediments is found to be very different from normal marine and non-marine shale mudrocks. This suggest that the previous method of establishing a normal trend by overlaying a number of porosity curves form offset wells will give wrong results if used in basins such as the North Sea.

1.4 Pressure, the basic concepts

Fluids differ from solids in that they are unable to support shear stress. When a body is submerged in a fluid such as water, the fluid exerts a force perpendicular to the surface at all locations around the surface of the body. If the body is small enough so we can neglect any differences in the vertical water column, the force (F) per unit area (A) is the same in all directions. This force per unit area is called the pressure P of the fluid:

$$P = F / A \quad [E1.1]$$

The SI unit of pressure is Newton per square meter (N/m^2), which is called Pascal (Pa). The equivalent imperial unit is pounds per square inch ($psi = lb/in^2$).

Liquids found in rocks in the subsurface are relatively incompressible. This means that the ratio of mass to volume, called density is approximately constant. For a liquid whose density is constant, the pressure increases linearly with depth. The pressure P at any point in a liquid column is:

$$P = P_0 + \rho \times g \times h \quad [E1.2]$$

P is the pressure at the surface and h is the vertical liquid column. The Greek letter ρ (rho) is the density. Density has the unit mass/volume ($kg/m^3 = g/cm^3$). g is the acceleration due gravity at the earth surface and equal to 9.81 m/s^2 .

Figure 1.5 shows a simplified diagram of how pore pressure may increase in a well. The hydrostatic pressure (often called the normal pressure) in sediments underlying the ocean often follows a gradient equal to 0.0101 MPa/m . That is the increase in hydrostatic pressure in water with an average density of 1.03 g/cm^3 . The overburden pressure is the pressure exerted by all overlying material, both solid and fluid. Below the water bottom, this line approximates 0.0226 MPa/m (1 psi/ft) in a clastic sedimentary environment. The pore pressure is the pressure of the fluid in the pore space of the rock. It may be equal to or higher than the hydrostatic pressure, but not higher than the overburden pressure (Figure 1.5). If the pore pressure approaches the overburden pressure the rock will fracture and release fluids. However, often fracturing will occur at a lower pressure, equivalent to the least principal stress, which

in an extensional basin is less than the overburden (the vertical stress). If at a specific depth of burial the mudrock permeability becomes so low that the excess water from normal compaction can no longer flow out of the system as fast as the rate of new sediments, the pore pressure will increase. The maximum increase of pore pressure by this mechanism called disequilibrium compaction (Swarbrick and Osborne, 1997)- and is often found to be parallel to the lithostatic gradient (Clayton and Hey, 1994), indicating, at depth, transfer of most/all of the load onto the pore fluid, with very little/no increase with vertical effective stress..

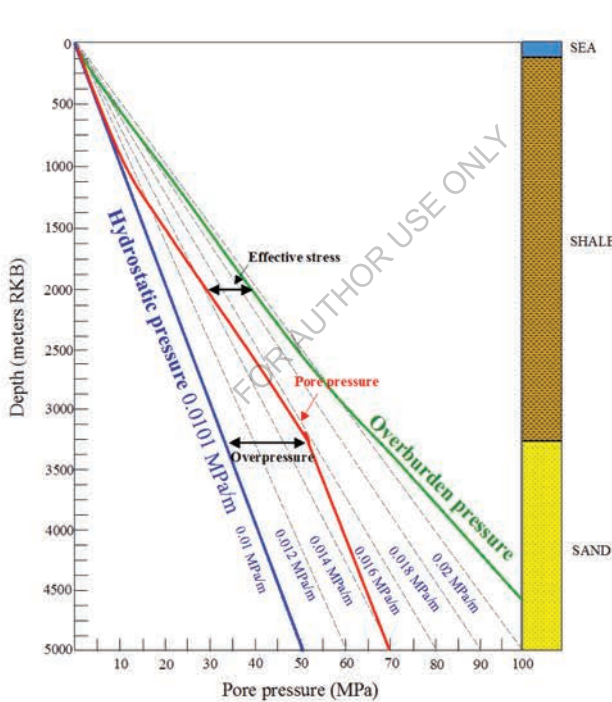


Figure 1.5 Pressure plotted against depth in a fictional well. The effective stress is equal to the overburden pressure minus the pore pressure and the overpressure is equal to the pore pressure minus the hydrostatic pressure.

In a borehole, the pressure exerted by the drilling fluid to either prevent influx of pore fluids from the formation or prevent hole caving instability is equivalent to

density of the drilling fluid and its column height. Therefore, the formation pore pressures are often converted into drilling fluid density equivalents so it is clear as what drilling fluid density just balances the pore pressures. Figure 1.6 shows how a typical pore pressure profile can be displayed as pressure gradient versus depth. If one follows the change in the pressure gradient of the pore pressure (red curve), every point on the curve represents a pressure gradient and a corresponding average fluid density that particular pressure at that depth represents. The maximum pore pressure gradient is reached at the top of the reservoir (3200 meters) equal 0.016 MPa/m. That is equivalent to the pressure at the bottom of a 3200-meter vertical fluid column with an average fluid density of 1.64 g/cm³. In exploration drilling a drilling mud is used where materials such as barite is mixed to form a liquid (called drilling mud) with such high average density. The terminology used is equivalent mud weight (EqMW). The pressure gradient plot illustrates a big challenge while drilling these wells. The EqMW has to be high enough to hold back the fluid from the depth where the formation has the highest-pressure gradient. However, in some formations, typically the shallower ones, this mud density would apply a pressure significantly greater than the pore pressures in these formations. This excess pressure may lead to fracturing of the rock and losses of the drilling fluid.

A confusing aspect in the oil industry with regard to pressure terminology is the mixing the terms; pressure gradient and density (EqMW). This becomes particularly difficult and confusing when working with a mixture of both imperial and the SI units. It has already been shown that the pressure gradient equals density multiplied by the acceleration due to gravity. In the imperial system, the norm is to use **weight density** rather than density. Weight density is defined as the ratio of the weight of an object to its volume. The units are pounds per gallon (ppg). As the weight is equal to the mass multiplied with gravity, both weight density and pressure gradient have the same units. The imperial unit system has historically been the norm in the oil industry and the people involved has become used to converting directly from weight density (ppg) to pressure gradient (psi/ft) and to pressure (psi). The word weight density is often shortened to density. This has created a problem when converting to the SI system. Too often, while converting from density (g/cm³) to pressure gradient (MPa/m), density is not multiplied by gravity (9.81 m/s²). A typical example is a recent paper titled “Pore Pressure terminology” in the Leading Edge written to explain

the problem, but failing to explain the difference between weight density and density (Bruce and Bowers, 2002).

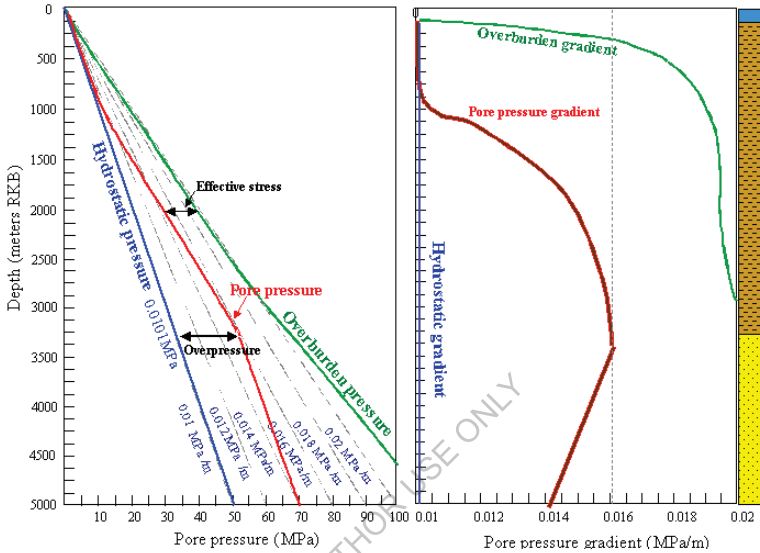


Figure 1.6 The Figure to the right shows how a pressure versus depth plot (left, Figure 1.5) becomes presented as pressure gradient versus depth.

1.5 Aims and layout of thesis

The aims and objective of this thesis are to:

1. Develop a critical review of current methods used to calculate the pore pressure in mudrocks.
2. Establish the uncertainties of the input variables using in principle component analysis, applied to the wireline measurements with reference to the mudrock porosity calculated and the drilling parameters with reference to the calculated drilling exponents.
3. Identify the variables that have the biggest impact on the estimation of pore pressure, and how they can be improved.

4. Compare the wireline signature of overpressured shales in the North Sea basin with those from the Gulf of Mexico.
5. Examine why the resistivity measurements of the mudrocks can be used as input parameter to calculate pore pressure in the Gulf of Mexico, while this has proved difficult to apply in the estimation of pore pressure in the North Sea.

Following the introduction comes Chapter 2 where the pressure concepts with respects to pore pressure in shallow sediments are discussed. That is followed by a discussion of mudrock porosity and normal compaction in mudrocks. Then the different pressure calculation methods, first with wireline logs as input, then those using drilling parameters.

Chapter 3 discusses the results from using these different pore pressure estimation methods on a test well, Nor 1/6-7 in the North Sea. The sensitivity of the input parameters are discussed. The results from the North Sea are then compared with the mudrocks from a mini-basin in the Gulf of Mexico,

Chapter 4 examines the glacial history of the North Sea to explain the nature of the shallow sediments, and their physical and petrophysical properties. Use of a novel application of the software Cyclog has helped in characterising the glacial sediments. Finally the relevance of the glacial history of the North Sea is reviewed in relation to the petroleum system which has generated productive oil and gas fields .